Extreme asymmetry of Néel domain walls in multilayered films of the dilute magnetic semiconductor (Ga,Mn)(As,P)

V. K. Vlasko-Vlasov, W.-K. Kwok, S. Dong, X. Liu, M. Dobrowolska, and J. K. Furdyna

Extreme asymmetry of Neel domain walls in multilayered films of diluted magnetic semiconductor (Ga,Mn)(As,P)

V. K. Vlasko-Vlasov and W.-K. Kwok,

Materials Sciences Division, Argonne National Laboratory, Argonne, Illinois 60439

S. Dong, X. Liu, M. Dobrowolska, and J. K. Furdyna

Department of Physics, University of Notre Dame, Notre Dame, Indiana 46556

We report on unconventional perfectly shaped, fully asymmetric $\sim 90^0$ Neel domain walls in multilayered films of the diluted ferromagnetic semiconductor (Ga,Mn)(As,P) with stepwise variation of P-doping. Our results contradict micromagnetic calculations, which favor symmetric domain walls due to crystallographic anisotropy and stray field energy. We demonstrate that both the puzzling uniaxial in-plane anisotropy in the tetragonal multilayered film and the asymmetry of the domain walls could result from Dzyaloshinskii-Moriya interactions that are enhanced by the multiple sharp interfaces between the layers and from anisotropic nonrelativistic exchange coupling. Our finding shows that digital variations of composition during the molecular beam epitaxy can be used to tune the anisotropy and chirality of magnetic multilayers.

Diluted magnetic semiconductors (DMSs) [1-5] are remarkable quantum materials that offer unique spintronics applications [6] and are full of surprises. In these materials, randomly distributed magnetic ions separated by tens of interatomic distances, interact

with the free charge carrier spins and transform a nonmagnetic matrix into a coherent ferromagnetic state. Although the basic physical origin of this state is qualitatively and in some cases semi-quantitatively understood in the framework of the Zener model [3-5], there are key open questions regarding the general magnetic properties of the DMSs, such as the value of its Curie temperature, exchange stiffness and magnetization, and puzzling magnetic anisotropy (see e.g. [5, 7]). In particular, there is no convincing explanation of the unusual in-plane uniaxial anisotropy that emerges from a presumably tetragonal DMS lattice [5, 8].

The majority of DMS samples are grown in the form of structurally perfect thin films using molecular-beam epitaxy (MBE), resulting in a homogeneous random distribution of magnetic ions. In such systems the induced strains due to the film/substrate lattice mismatch strongly affect the anisotropy of the sample through magnetoelastic effects and interfacial interactions. The in-plane or perpendicular orientation of their easy magnetization axes will depend on the composition, resulting in a compressed or stretched film. Furthermore, the crystal symmetry of the DMS can contribute to the anisotropy through strong spin-orbit coupling in the valence band holes mediating magnetic ordering.

An important component of the DMS film anisotropy can result from the symmetry breaking at the film/substrate interface, where the same strong spin-orbit coupling introduces a chirality due to lost inversion symmetry and consequent Dzyaloshinskii-Moriya interactions (DMI) [9]. These interfacial antisymmetric interactions can promote a unidirectional magnetization twist that generates new types of magnetic structures, such as skyrmions and Dzyaloshinskii domain walls with preferred chirality and reduced energy (see [10] and references therein). However, the interfacial DMI is essential only in very thin

2

films. In this work, we amplify the effect of the interfacial DMI by introducing multiple interfaces in the DMS film, (GaMn)(AsP), with digitally modulated content of phosphorus. The main result is the realization of a perfect domain structure with well-defined, entirely asymmetric Neel domain walls (DWs). These DWs cannot be explained with conventional micromagnetic calculations [11] using experimentally found magnetic parameters. We argue that they result from the chiral anisotropy of the films associated with their multilayered structure, which yields a cumulatively amplified DMI and are possibly sustained by the anisotropic nonrelativistic exchange interaction in Mn doped GaAs.

We grew graded multilayers of $(Ga_{0.93}Mn_{0.07})As_{1-x}P_x$ using low-temperature MBE with stepwise changes of the phosphorus concentration from x =0.03 to 0.28. The resulting 100 nm films have sharp interfaces between eight 12.5nm layers with different x as revealed by high-resolution TEM images (Fig.1s in Supporting information). The magnetization of the as-grown film is mainly determined by the Mn content, which was fixed during growth, and only weakly depends on x [12]. Since the individual layer thickness is smaller than the exchange length $l_{ex}=[A/2\pi M_s^2]\sim17$nm (with the exchange constant $A\sim10^{-8}$ erg/cm [9] and our measured saturation magnetization $M_s(T=5K) =24$ emu/cm^3), there is strong magnetic coupling between layers. Consequently, the films were in a homogeneous magnetic state, as confirmed by our macroscopic magnetization loop measurements, magnetoresistance, and anomalous Hall data, which yielded a single Curie temperature, $T_c = 52$K, and no heterogeneous features.

At low temperatures ($T<<T_c$) our films have two easy axes (EA) tilted by a small angle α from [100] and [010] towards [110]. This is a typical feature of compressively strained (Ga,Mn)As films grown by MBE on (001)GaAs substrates, where α increases with

temperature, resulting in a uniaxial state with EA||[110] at $T > T_c/2$ [1-5]. Adding phosphorus introduces tensile strains [13, 14] and promotes the out-of-plane easy axis at x > 0.07 for Mn concentrations ~4-6% [15,16]. However, in our multilayered films, where the P-concentration increases in small steps, the average stresses are reduced and the magnetization remains in the film plane, while retaining the ubiquitous [110] uniaxial *in-plane* anisotropy.

The emergence of uniaxial anisotropy along [110] in tetragonal films is a controversial issue that has so far eluded a convincing explanation. Possible reasons include the preferred arrangement of Mn ions owing to surface reconstruction in GaAs [17-18], formation of Mn-pairs along [110] [8, 19], interfacial DMI effect [9], anisotropic exchange [20], or unidirectional film surface modulation [21]. In our samples, we find that the uniaxial anisotropy, which drives the easy axes to tilt from the cubic [100] and [010] towards [110], is directly imprinted onto the emergent domain patterns. We argue that the observed unusual DW alignment results from the DMI effect enhanced by multiple interfaces in our multilayered films.

To visualize the domains, we used a magneto-optic (MO) indicator technique [22], which detects stray fields H_s of the DWs at the sample surface. The weak contrast at the DWs (due to small $H_s \sim M_s$) is enhanced using an image subtraction technique, whereby MO images of an initially polarized reference state are subtracted from subsequent images of emerging domain states. Furthermore, to control the magnetization direction in the domains, we lithographically fabricated apertures in the film in the shape of a long slit and a set of 150 μm x 150μm squares with edges aligned with the [100] and [010] directions (see

Fig.1). The stray fields at the edges of the apertures are proportional to the magnetization components perpendicular to the edges (M_n), and reveal changes of M_n in expanding domains.

Initially, we apply and switch off an in-plane field of H_a =1kOe along one of the {100} directions, which polarizes the sample along the easy axis, closest to the $\mathbf{H_a}$ direction. At T=5K there are two easy axes, EA1 and EA2, tilted by $\alpha \sim 5^0$ from [100] and [010] (see Fig. 1d). Following the initial polarization, we either applied field along a perpendicular direction (*perpendicular remagnetization*), or ramped H_a between positive and negative values along the initial direction (*axial remagnetization*).

In the polarized state the stray fields along the edges of the sample and apertures appear as bright and dark contrast on the MO image. After subtraction of this polarized-state image from subsequent images obtained with different $\mathbf{H_a}$ directions, the boundaries of the emerging domains with stray fields of different signs can be promptly seen in the difference images as soon as the remagnetization process begins (Fig1. a, b). In turn, contrast on the apertures appears when new domains expand to the edges of the apertures (Fig. 1c), thus altering their M_n, as sketched in Fig. 1f.

Fig.1a shows an MO image of domains emerging during *perpendicular remagnetization* of the sample. The initial state has magnetization $\mathbf{M_1}$ || –EA1. After application of $\mathbf{H}$||[010], new domains appear with $\mathbf{M_2}$||EA2. These domains have the shape of rhombuses with well-defined DWs along EA1 and EA2 (Fig.1a-b). The only exceptions are domains nucleated at scratches in the sample (yellow lines in Fig.1a-b), which expand initially with a sawtooth pattern. Eventually, the domains grow and merge, but their boundaries always remain along EA1 and EA2 (Fig.1c). All the DWs complete *$90^0+2\alpha$*

counter-clockwise (CCW) magnetization twist (going from M_2 to M_1). This is defined by the direction of the initial magnetization and the applied field. Starting with the same initial $M_1||-EA1$, but applying $H||[0-10]$, results in similar domain patterns with DWs along EA1 and EA2, albeit with *90^0-2α* clockwise (CW) domain walls (Fig.5s in Supplemental Information [23]).

During the *axial remagnetization* of the sample, we observe two stages of domain nucleation and growth (Fig.2). The domains appear in well separated narrow field ranges, where the first stage DWs have always 90^0-2α angle while the 90^0+2α DWs appear during the second stage at higher fields. Such a two-stage twist of the magnetization is a common feature in films with biaxial in-plane anisotropy (see [24, 17-18]). In our case, the smaller 90^0-2α angle twist always appears first, which suggests a smaller nucleation barrier E_B for the 90^0-2α domains (see other effects of E_B in the Supplemental information [23]). In the presence of DMI, its effect should be smaller than the difference between E_B for the 90^0-2α and 90^0+2α domain nucleation, but it will still contribute to the energy of the DWs, as discussed below.

The bright and dark contrast of the DWs in Figs.1 and 2 reveals the stray fields H_s corresponding to positive and negative magnetic charges ρ_m at the DWs (see Fig.1e and Fig.2c-d). They appear due to gradients of the magnetization component M_n normal-to-the-DW-plane (ρ_m=-div$M$=-dM_n/dn). In Bloch walls, the charges would also emerge due to a tilt of M from the film surface, but for the Neel DWs expected in our samples (e.g. [25-26]), such a surface component will be absent, unless it is induced by DMI (see below). Magnetic charges inside DW are a hallmark of Neel walls. However, in the symmetric Neel DWs (Fig.3a) with equal M_n in the neighboring domains, the sign of ρ_m alternates, yielding a net

charge of zero. This reduces the range of H_s and the resulting magnetostatic energy E_{ms}. In asymmetric Neel DWs (Fig. 3 b), ρ_m has one sign, extending the range of H_s and increasing E_{ms}. The 90-2α (or 90+2α) DWs parallel to EA1 or EA2 represent the extreme asymmetric case with maximum E_{ms}. A higher E_{ms} can be only in the so-called head-to-head DWs that appear under special conditions, e.g. under strong magnetic field gradients. In traditional magnetic materials with significant $2\pi M_s^2$, the 90^0 DWs of different types (Bloch, Neel, cross-tie) are symmetric for both bulk and thin films (e.g. [27-31]) in order to minimize E_{ms}. Symmetric 90^0 DWs were observed also in (Ga,Mn)As films (see Fig.1 and 4 in[25 and 26]). We found only one example of strongly corrugated 90^0 DWs with average orientation along one of the easy axes, observed in ultrathin cobalt films on Cu(100) (Fig.4 in [32]). Also, DWs oriented at uneven angles to the easy axes were visualized in narrow (GaMn)As Hall bars [33], although the reason was not discussed.

The ultimate asymmetry of the domain walls revealed in Figs.1-2 is highly unusual and does not follow from common micromagnetic analysis described below. Accounting that M_s in our sample is small, their dominant biaxial in-plane anisotropy strongly suggests *in-plane* rotation of **M**, hence favoring the Neel DW structure. We calculated the structure and energy of the 90^0-2α Neel DWs as a function of their orientation, admitting the exchange and cubic and uniaxial in-plane anisotropy terms, but neglecting E_{ms}. Then we estimated the magnetostatic contribution to the wall energy.

Minimizing the total DW energy yields (see details in the Supplemental Information [23]):

$$\frac{y}{\Delta} + C = \frac{1}{2\sqrt{1-\beta^2}} ln \frac{\sqrt{1-\beta^2}+(\beta u-1)}{\sqrt{1-\beta^2}-(\beta u-1)} \tag{1}$$

Here y is the coordinate along the DW normal, $\Delta=(A/K_c)^{1/2}$, A is the exchange constant, $\beta=$ $K_u/4K_c =\sin 2\alpha$, K_c and K_u are the cubic and [110] uniaxial anisotropy constants, $u= tg(\varphi+\varphi_w)$, φ is the angle between **M** and y, φ_w is the angle between y and [100], and $C(\varphi_w)$ gives the position of the DW, which can be chosen e.g. as y=0 at $\varphi+\varphi_w =\pi/4$, i.e. u=1 in (1).

From (1) we find that the DW energy (neglecting E_{ms}) does not depend on the DW orientation φ_w. Since the small E_{ms} hardly alters the DW structure, we calculate the magnetostatic energy using the solution (1) for 90^0-2α DW and find that it has a minimum for $\varphi_w=\pi/4$, i.e. for the symmetric DWs (Fig.8s in Supplemental Information [23]).

Above analysis accounts for the isotropic exchange stiffness, A, as commonly assumed in micromagnetic treatment of (Ga,Mn)As [34-36]. However, many first principle calculations show that the exchange constants in zinc-blende DMS structure may be *anisotropic*, which holds when neglecting spin-orbit coupling (SOC) [36-38], and is even more robust if SOC is taken into account [20, 38, 40, 41, 6]. Although not very large, the exchange anisotropy could affect the alignment of the DWs in our sample. By introducing the anisotropic exchange constant in (1) with the same angular dependence as the magnetic anisotropy E_A, $A\sim \sin^2 2\varphi_w+(K_u/K_c)\sin^2(\varphi_w -\pi/4)$ the DW energy $\varepsilon_{DW}\sim A^{1/2}$ will be a minimum for the DW orientation exactly along the easy axes in our films. Since anisotropic exchange was already shown to control the DW orientation in thin iron films on W(110) substrates [42], a similar effect could exist in DMS films.

However, in single layer (GaMn)As films, the easy axis orientation of 90^0 DWs has not been observed (e.g. [25-26]). We assume that the asymmetric DW alignment found in our multilayer sample is defined by to the interfacial interactions enhanced by the presence of multiple interfaces. According to Ref. [9], the broken inversion symmetry at the

GaAs(001)/(Ga,Mn)As interface results in an asymmetric Dzyaloshinskii-Moriya coupling $\mathbf{D}_i$ ($\mathbf{m} \times d\mathbf{m}/d\mathbf{r}_i$) [43-45], where $\mathbf{D}_i$ is the Dzyaloshinskii vector defined by the crystal symmetry, $\mathbf{m} = \mathbf{M}/M$, and $d\mathbf{m}/dr$ is its spatial derivative. This interfacial DMI may introduce uniaxial [110] anisotropy in thin films [9]. E.g. it forces Neel-type DWs of preferred chirality in films with perpendicular anisotropy [46-50], where the direction of $\mathbf{D}$ at the interface between magnetic layers and a nonmagnetic substrate with large SOC is parallel to the interface and normal to the spin rotation axis. In our samples, the DMI between interfacial Mn spins also should be mediated by strong SOC effects in the GaAs structure, and following the Moriya symmetry rules [45] (see [46, 9,51]) we should assume that the $\mathbf{D}$ vector is along (001) zinc-blende plane and perpendicular to the DW. In the Neel wall between the in-plane domains, $\mathbf{m} \times d\mathbf{m}/dr$ is perpendicular to the film and the DMI effect should vanish. However, it turns out that the same DMI can modify the Neel DW by introducing a small *out-of–plane* twist of $\mathbf{M}$ [52, 53]. Although the DMI changes the DW structure only slightly, it contributes to the DW energy and stabilizes the DWs with one chirality of the out-of-plane twist. So far this has been shown for 180^0 Neel DWs [52, 53], but similar DMI effect may be realized for $\sim 90^0$ DWs in our films. Appropriate sketch of the magnetization twist in the DWs around a nucleating domain is shown in Fig.4.

The DMI may be amplified in our multilayered films. Stochastically distributed Mn ions can be placed on the same GaAs matrix at the interfaces and experience the same DMI, such that the total effect increases with the number of interfaces. The amplified DMI effect coupled with the anisotropic exchange interactions will support the uniaxial in-plane anisotropy, as suggested in [9], and may cause the observed robust asymmetry of the $90^0 - 2\alpha$ and $90^0 + 2\alpha$ DWs in our films.

We note that DMI can also be anisotropic, as it was reported recently for thin Au/Co/W(110) and Fe/W(110) films, where the Dzyaloshinskii coefficients D was several times different along symmetry directions [54-55]. In this case, the preferred DW orientation should be perpendicular to the direction l of maximum D, yielding the minimum DW energy due to the out-of-plane chiral twist of $\mathbf{M}$ around l. In our experiment, it is hard to distinguish fields due to the out-of-plane component (M_z) in the DW from the fields of strong magnetic charges inside the asymmetric Neel DW. However, the bright and dark DW contrast in Fig.1-2 could contain a small contribution from M_z as suggested in Fig.4.

In conclusion, we have imaged the low temperature domain structure in multilayered films of the dilute ferromagnetic semiconductor (Ga,Mn)(As,P) with digitally modulated content of P and discovered unique fully asymmetric Neel domain walls in these samples. Such extreme asymmetry is in contrast with the magnetostatic contribution to the DW energy calculated based on the symmetric exchange stiffness and cubic and uniaxial anisotropy terms. We propose that the interfacial Dzyaloshinskii-Moriya interactions in our multilayer sample, and possibly the nonrelativistic anisotropic exchange coupling, could be responsible for the observed unusual Neel DW alignment. The robust orientation of the DWs imprints a specific anisotropy induced by the broken symmetry at the multilayer interfaces and amplified by their multiple repetition. The stepwise variations of composition during MBE growth could be a useful tool for tuning the anisotropy and chirality of magnetic films.

References

[1] J. K. Furdyna, *Diluted magnetic semiconductors* , J. Appl. Phys. **64**, R29 (1988)

[2] W. Prellier, A Fouchet and B Mercey, *Oxide-diluted magnetic semiconductors: a review of the experimental status*, J. Phys.: Cond. Matt. **15**, R1583 (2003)

[3] T. Jungwirth, J. Sinova, J. Masek, J. Kucera, and A. H.MacDonald, *Theory of ferromagnetic (III,Mn)V semiconductors*, Rev. Mod. Phys. **78**, 809 (2006).

[4] K. Sato, L. Bergqvist, J. Kudrnovsky´, P.H. Dederichs, O. Eriksson, I. Turek, B. Sanyal, G. Bouzerar, H. Katayama- Yoshida, V. A. Dinh, T. Fukushima, H. Kizaki, and R. Zeller, *First-principles theory of dilute magnetic semiconductors,* Rev. Mod. Phys. **82**, 1633 (2010).

[5] T. Dietl and H. Ohno , *Dilute ferromagnetic semiconductors: Physics and spintronic structures* ,Rev. Mod. Phys. **86**, 187 (2014).

[6] T. Jungwirth, J. Wunderlich, V. Novak, K. Olejnik, B. L. Gallagher, R. P. Campion, K. W. Edmonds, A. W. Rushforth, A. J. Ferguson, P. Nemec, *Spin-dependent phenomena and device concepts explored in (Ga, Mn) As*, Rev. Mod. Phys. **86** , 855 (2014).

[6b] Kapetanakis, M. D., I. E. Perakis, K. J.Wickey, C. Piermarocchi, and J. Wang, "**Femtosecond coherent control of spins** in (Ga,Mn) As ferromagnetic semiconductors using light," Phys. Rev. Lett. **103**, 047404 (2009). <<applications>>

[7] H. Puszkarski, P.Tomczak, *Spin-wave resonance as a tool for probing surface anisotropies in ferromagnetic thin films: Application to the study of (Ga,Mn)As* , Surf. Sci. Rep.**72**, 351 (2017).

[8] M. Birowska, *Influence of the different strains' components on the uniaxial magnetic anisotropy parameters for a (Ga,Mn)As bulk system: A first-principles Study*. J. Magn. Magn. Mater. **432**, 396 (**2017).**

[9] A. Werpachowska, T. Dietl, *Theory of spin waves in ferromagnetic (Ga,Mn)As* , Phys. Rev. B **82**, 085204 (2010) .

[10] F. Hellman, A. Hoffmann, Y. Tserkovnyak, G. S. D. Beach, E. Fullerton, C. Leighton, A. H. MacDonald, D. C. Ralph, D. A. Arena, H. A. Durr, *Interface-induced phenomena in magnetism*, Rev. Mod. Phys. **89**, 025006 (2017)   <906 refs>

[11] L.D. Landau and E.M. Lifshitz, *Electrodynamics of continuous media*, Oxford, New York : Pergamon, 1984

[12] X. Li, X. Liu, S. Dong, C. Gorsak, J. K. Furdyna, M. Dobrowolska, S.-K. Bac, S. Lee, S. Rouvimov, *Dependence of ferromagnetic properties on phosphorus concentration in $Ga_{1-x}Mn_xAs_{1-y}P_y$* , J. Vac. Sci. Technol. **36**, 02D104 (2018)

[13] M. Cubukcu, H. J. von Bardeleben, Kh. Khazen, J. L. Cantin, O. Mauguin, L. Largeau, A. Lemaitre, *Adjustable anisotropy in ferromagnetic (Ga,Mn) (As,P) layered alloys* , Phys. Rev. B **81**, 041202 (2010).

[14] L. Thevenard, E. Peronne, C. Gourdon, C. Testelin, M. Cubukcu, E. Charron, S. Vincent, A. Lemaitre, and B. Perrin , *Effect of picosecond strain pulses on thin layers of the ferromagnetic semiconductor (Ga,Mn)(As,P)* , Phys. Rev. B **82**, 104422 (2010).

[15] M. Yahyaoui, K. Boujdaria, M. Cubukcu, C. Testelin, C. Gourdon, *The influence of phosphorus content on magnetic anisotropy in ferromagnetic (Ga, Mn) (As, P)/GaAs thin films*, J. Phys.: Condens. Matter **25**, 346001 (2013).

[16] X. Liu, X. Li, S.-K. Bac, X. Zhang, S. Dong, S. Lee, M. Dobrowolska, and J. K. Furdyna, *Ferromagnetic resonance and spin-wave resonances in GaMnAsP films*, AIP Adv. **8**, 056402 (2018).

[17] U. Welp, V. K. Vlasko-Vlasov, T. Wojtowicz, X. Liu, and J. K. Furdyna, *Magnetic Domain Structure and Magnetic Anisotropy in Ga$_{1-x}$Mn$_x$As*, Phys. Rev. Lett. **90**, 167206 (2003).

[18] U. Welp, V. K. Vlasko-Vlasov, A. Menzel, and H. D. You, X. Liu, J. K. Furdyna, T. Wojtowicz, *Uniaxial in-plane magnetic anisotropy of Ga$_{1-x}$Mn$_x$As*, Appl. Phys. Lett. **85**, 260 (2004).

[19] M. Birowska,1 C. Sliwa,2 J. A. Majewski,1 and T. Dietl, *Origin of Bulk Uniaxial Anisotropy in Zinc-Blende Dilute Magnetic Semiconductors*, Phys. Rev. Lett. **108**, 237203 (2012).

[20] C. Timm, A. H. MacDonald, *Anisotropic exchange interactions in III-V diluted magnetic semiconductors*, Phys. Rev B **71**, 155206 (2005).

[21] S. Piano, X. Marti, A. W. Rushforth, K. W. Edmonds, R. P. Campion, M. Wang, O. Caha, T. U. Schulli, V. Holy, and B. L. Gallagher, *Surface morphology and magnetic anisotropy in (Ga,Mn)As*, Appl. Phys.Lett. **98**, 152503 (2011).

[22] V. K. Vlasko-Vlasov, G. W. Crabtree, U. Welp, and V. I. Nikitenko, Magneto-optical studies of magnetization processes in high-Tc superconductors, NATO ASI Ser., Ser. E **356**, 205 (1999).

[23] Supplemental Information for this work presents macroscopic magnetization and transport measurements, additional images of the domain structure, and details of the micromagnetic calculations.

[24] R. P. Cowburn, S. J. Gray, J. Ferre, J. A. C. Bland, J. Miltat, *Magnetic switching and in-plane uniaxial anisotropy in ultrathin Ag/Fe/Ag(100) epitaxial films*, J. Appl. Phys. **78**, 7210 (1995).

[25] A. Sugawara, H. Kasai, A. Tonomura, P. D. Brown, R. P. Campion, K.W. Edmonds, B. L. Gallagher, J. Zemen, and T. Jungwirth, *DomainWalls in the (Ga,Mn)As Diluted Magnetic Semiconductor*, Phys. Rev. Lett. **100**, 047202 (2008).

[26] A. Sugawara, T. Akashi, P. D. Brown, R. P. Campion, T. Yoshida, B. L. Gallagher, A. Tonomura, *High-resolution observations of temperature-dependent magnetic domain structures within $Ga_xMn_{1-x}As$ by Lorentz microscopy*, Phys. Rev. B **75**, 241306 (2007).

[27] E. Gu, J. A. C. Bland, C. Daboo, M. Gester, L. M. Brown, R. Ploessl and J. N. Chapman, *Microscopic magnetization reversal processes and magnetic domain structure in epitaxial Fe/GaAs(001) films*, Phys. Rev. B **51**, 3596 (1995).

[28] A. Hubert, R. Schafer, *Magnetic Domains*, Berlin-Heidelberg-New York: Springer-Verlag. (1998).

[29] P. Leinenbach, J. Losch, U. Memmert, U. Hartmann, *Ultrahigh vacuum magnetic force microscopy on in situ grown iron thin films*, Appl. Phys. A **66**, S1191 (1998).

[30] J. L. Costa-Kramer, D. M. Borsa, J. M. Garcia-Martin, M. S. Martin-Gonzalez, D. O. Boerma, F. Briones, *Structure and magnetism of single-phase epitaxial γ'-Fe_4N*, Phys. Rev. B 69, 144402 (2004).

[31] V. P. Panaetov, *Experimental Investigation of the Magnetic Structure of Domain Walls in Thin Ferromagnetic Films* , Phys. Sol. State 51, 2064 (2009) (orig.- Fiz. Tverd. Tela, **51**, 1946 (2009)).

[32] H.P. Oepen, *Magnetic domain structure in ultrathin cobalt films*, J. Magn, Magn. Mat. **93**, 116 (1991).

[33] J. Honolka, L. Herrera Diez, R. K. Kremer, K. Kern, E. Placidi, F. Arciprete, *Temperature-dependent Neel wall dynamics in GaMnAs/GaAs*, New J. Phys. 12, 093022 (2010).

[34] X. Liu, Y. Y. Zhou, J. K. Furdyna, *Angular dependence of spin-wave resonances and surface spin pinning in ferromagnetic (Ga,Mn) As films*, Phys. Rev. B 75, 195220 (2007).

[35] N. Tesarova, D. Butkovicova, R. P. Campion, A. W. Rushforth, K. W. Edmonds, P. Wadley, B. L. Gallagher, E. Schmoranzerova, F. Trojanek, P. Maly, P. Motloch, V. Novak, T. Jungwirth, and P. Nemec, *Comparison of micromagnetic parameters of the ferromagnetic semiconductors (Ga,Mn)(As,P) and (Ga,Mn)As*, Phys. Rev. B **90**, 155203 (2014).

[36] H. Puszkarski, P. Tomczak, *Spin-wave resonance as a tool for probing surface anisotropies in ferromagnetic thin films: Application to the study of (Ga,Mn)As* , Surf. Sci. Rep. **72**, 351 (2017).

[37] J. Kudrnovsky, I. Turek, V. Drchal, F. Maca, P. Weinberger, and P. Bruno, *Exchange interactions in III-V and group-IV diluted magnetic semiconductors*, Phys. Rev. B **69**, 115208 (2004).

[38] H. Ebert, S. Mankovsky, *Anisotropic exchange coupling in diluted magnetic semiconductors: Ab initio spin-density functional theory*, Phys. Rev B **79**, 045209 (2009).

[39] K. Sato, L. Bergqvist, J. Kudrnovský, P. H. Dederichs, O. Eriksson, I. Turek, B. Sanyal, G. Bouzerar, H. Katayama-Yoshida, V. A. Dinh, T. Fukushima, H. Kizaki, R. Zeller, *First-principles theory of dilute magnetic semiconductors*, Rev. Mod. Phys. **82**,1633 (2010).

[40] S. Mankovsky, S. Polesya, S. Bornemann, J. Minar, F. Hoffmann, C. H. Back, H. Ebert, *Spin-orbit coupling effect in (Ga,Mn)As films: Anisotropic exchange interactions and magnetocrystalline anisotropy*, Phys. Rev. B **84**, 201201 (2011).

[41] T. Kernreiter, *RKKY interaction induced by two-dimensional hole gases*, Phys. Rev. B 88, 085417 (2013).

[42] E.Y. Vedmedenko, A. Kubetzka, K. von Bergmann, O. Pietzsch, M. Bode, J. Kirschner, H. P. Oepen, and R.Wiesendanger, *Domain Wall Orientation in Magnetic Nanowires*, Phys. Rev. Lett. **92**, 077207 (2004).

[43] I. Dzyaloshinsky, *A thermodynamic theory of "weak" ferromagnetism of antiferromagnetics*, J. Phys. Chem. Solids **4**, 241 (1958).

[44] I. E. Dzyaloshinskii, *Theory of helicoidal structures in antiferromagnets. I. Nonmetals*, Sov. Phys. JETP **19**, 960 (1964). (orig.: Zh. Exp. Teor. Fiz. **46**, 1420 (1964)).

[45] M. Moriya, *Anisotropic Superexchange Interaction and Weak Ferromagnetism*, Phys. Rev. 120, 91 (1960).

[46] M. Heide, G. Bihlmayer, and S. Blugel, *Dzyaloshinskii-Moriya interaction accounting for the orientation of magnetic domains in ultrathin films: Fe/W(110)*, Phys. Rev. B 78, 140403 (2008).

[47] Gy. J. Vida, E. Simon, L. Rozsa, K. Palotas, and L. Szunyogh. *Domain-wall profiles in Co/Irn/Pt(111) ultrathin films: Influence of the Dzyaloshinskii-Moriya interaction*, Phys. Rev. B **94**, 214422 (2016).

[48] A. Thiaville, S. Rohart, E. Jue , V. Cros, A. Fert, *Dynamics of Dzyaloshinskii domain walls in ultrathin magnetic films*, Euro. Phys. Lett. **100**, 57002 (2012).

[49] M.J. Benitez, A. Hrabec, A.P. Mihai, T.A. Moore, G. Burnell, D. McGrouther, C.H. Marrows, S. McVitie, *Magnetic microscopy and topological stability of homochiral Neel domain walls in a Pt/Co/AlO$_x$ trilayer*, Nat. Comm. 6, 8957 (2015).

[50] C. B. Muratov, V. V. Slastikov, A. G. Kolesnikov, O. A. Tretiakov, *Theory of the Dzyaloshinskii domain-wall tilt in ferromagnetic nanostrips*, Phys. Rev. B **96**, 134417 (2017).

[51] H. Yang, A. Thiaville, S. Rohart, A. Fert, M. Chshiev, *Anatomy of Dzyaloshinskii-Moriya Interaction at Co/Pt Interfaces*, Phys. Rev. Lett. **115**, 267210 (2015).

[52] V. P. Kravchuk , *Influence of Dzialoshinskii–Moriya interaction on static and dynamic properties of a transverse domain wall*, J. Magn. Magn. Mater. **367**, 9 (2014).

[53] S.-W. Lee , B.-G. Park , K.-J. Lee, *Fast current-induced motion of a transverse domain wall induced by interfacial Dzyaloshinskii-Moriya interaction*, Curr. Appl. Phys.**15**, 1139 (2015).

[54] L. Camosi, S. Rohart, O. Fruchart, S. Pizzini, M. Belmeguenai, Y. Roussigné, A. Stashkevich, S. M. Cherif, L. Ranno, M. de Santis, J. Vogel, *Anisotropic Dzyaloshinskii-Moriya interaction in ultrathin epitaxial Au/Co/W(110)*, Phys. Rev. B **95**, 214422 (2017).

[55] M. Hoffmann, B. Zimmermann, G. P. Muller, D. Schurhoff, N. S. Kiselev, C. Melcher, S. Blugel, *Antiskyrmions stabilized at interfaces by anisotropic Dzyaloshinskii-Moriya interactions*, Nat. Comm. **8**, 308 (2017).
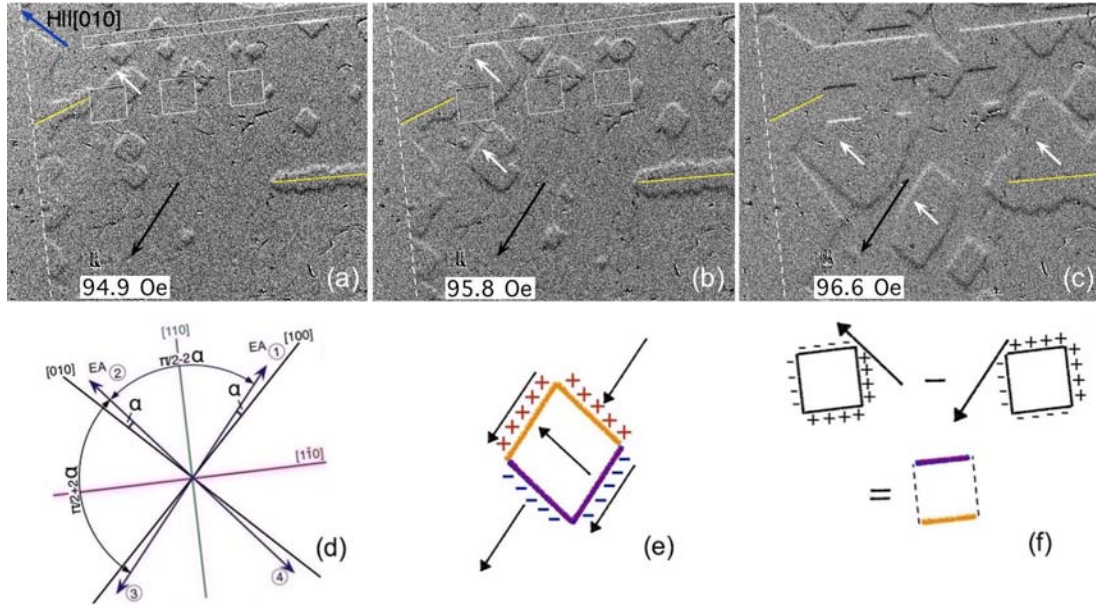
Figures

Fig.1 Magneto-optical images of the nucleation and growth of domains during perpendicular remagnetization at T=5K (a-c). The orientation of the easy axes EA1 and EA2 and the crystal axes is shown in (d). The sample has 3 etched 150x150 μm square apertures and a slit with sides parallel to [110] and [1-10] (white lines). The yellow lines indicate scratches in the sample. The sample is initially polarized into a monodomain state (not shown) with $M_1 \|$–EA1 (black arrow) by application of H=1kOe$\|$[-100] and switching off H. Panels (a-c) present subsequent images in $H\|$[010] after subtraction of the initial polarized M_1-state picture to enhance the contrast of new domains. Rhombus-shaped domains with $M_2 \|$ EA2 (white arrows) appear and grow with increasing H. They have bright and dark $90^0+2\alpha$ domain walls (DWs) oriented along EA1 and EA2. Domains nucleating at the scratches have zigzag boundaries. The DW bright and dark contrast reveals Up and Down directed stray fields due to + and - magnetic charges at the DWs (e). Visualization of the stray fields at the edges of the apertures allows monitoring of the M components in adjoining areas. In the subtracted image (c), the square aperture and the slit sides where the magnetic charge inverts sign, become visible upon the expansion of M_2 domains as sketched in (f). Our MOI resolution is ~2μm, but the stray fields diverge in a range wider than 2μm.
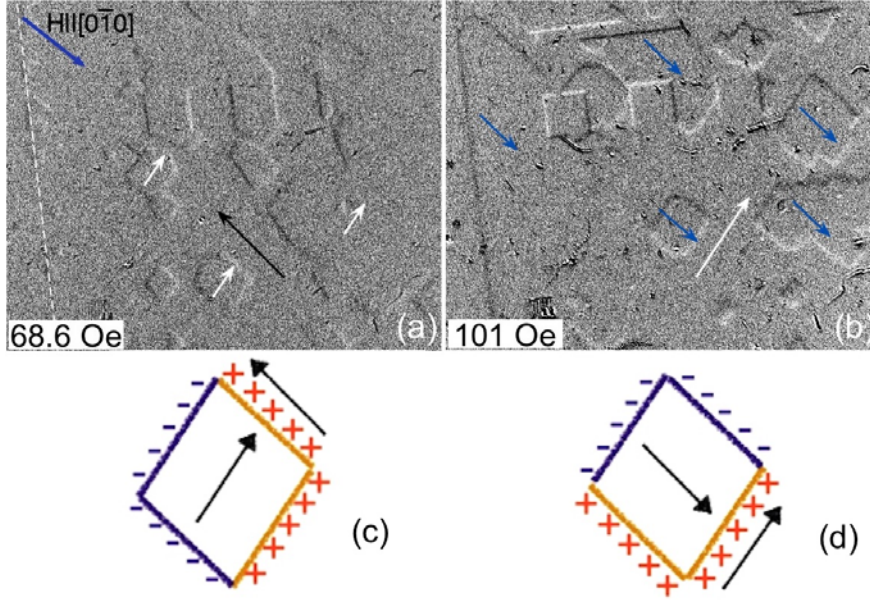
18

Fig.2. (a-b) Magneto-optical images of two-stage axial remagnetization at T=5K. Images of the same area as in Fig.1 are referenced to the initial monodomain M_1-state with $M_1||EA_2$ (black arrow) formed after application of $H||[010]$. Subsequent application of $H||[1-10]$ promotes nucleation and growth of domains with $M_2 ||EA1$ (white arrows) (a). These domains have bright and dark boundaries associated with magnetic charges sketched in (c). In this first remagnetization stage, the M_2 domains have $90^0-2\alpha$ DWs. At larger H, the M_2 domains expand and form a monodomain state (not shown) where then new domains with $M_3 ||-EA2$ (blue arrows) appear and grow (b). These domains have bright and dark bottom and top-side boundaries associated with the magnetic charges sketched in (d). In the second rotation stage, the M_3 domains have $90^0+2\alpha$ DWs. For both stages the DWs are oriented along EA1 and EA2.
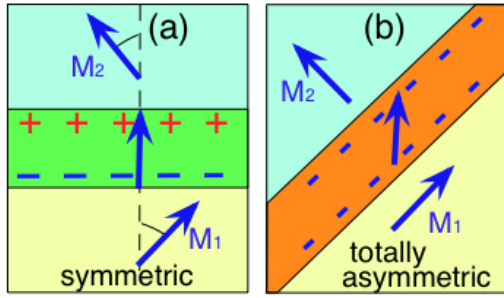
Fig.3 Sketch of symmetric and asymmetric 90^0 Neel domain walls. In the symmetric case (a), magnetic charges ρ_m changes sign across the DW, whereas they have one sign in the asymmetric Neel wall (b). Details of the ρ_m distribution are presented in the Supplemental information [23]. The range of stray fields H_s for (b) is much larger, similar to H_s of a charged line decaying with distance as $1/R$, compared to a dipole of +/- lines with $H_s \sim 1/R^2$ in (a). Blue arrows show magnetization vectors in the domains and inside the Neel DW.
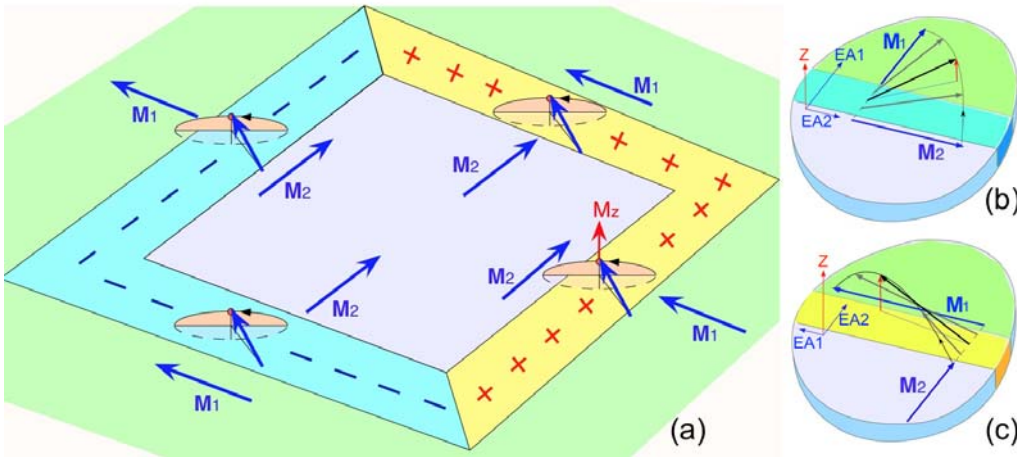

Fig.4 Sketch of asymmetric Neel domain walls modified by Dzyaloshinskii-Moriya interactions. $\mathbf{M}_1 \parallel EA_1$ in the initial state and $\mathbf{M}_2 \parallel EA_2$ in the nucleating domain are both in the film plane. Due to the DMI, magnetization in the Neel DW tilts slightly out of the plane, as shown by ellipses with their small axis along the film normal Z. Within the DWs, **M**

rotates in the film plane and out of plane as shown in (b) and (c). Magnetic charges in the DWs shown by + and - are defined by the asymmetric in-plane rotation of $\mathbf{M}$, while the M_z contribution is small. All the DWs around the nucleating domain have the same CCW chirality for rotation from $\mathbf{M}_2$ to $\mathbf{M}_1$.